Обзор ArXiv/astro-ph, 25-30 ноября 2025

От Сильченко О.К.

ArXiv: 2511.19632

Disc growth and vertical heating of lenticular galaxies in the Fornax cluster

Marie Martig[1★], Francesca Pinna[2,3], Jesús Falcón-Barroso[2,3], Ignacio Martín-Navarro[2,3], Ivan Minchev[4], Yuchen Ding[1]
[1]Astrophysics Research Institute, Liverpool John Moores University, 146 Brownlow Hill, Liverpool L3 5RF, UK
[2]Instituto de Astrofísica de Canarias, Calle Via Láctea s/n, 38200 La Laguna, Tenerife, Spain
[3]Depto. Astrofísica, Universidad de La Laguna, Calle Astrofísico Francisco Sánchez s/n, 38206 La Laguna, Tenerife, Spain
[4]Leibniz-Institut für Astrophysik Potsdam (AIP), An der Sternwarte 16, D-14482 Potsdam, Germany

Accepted XXX. Received YYY; in original form ZZZ

ABSTRACT
We present a detailed analysis of the vertical and radial structure of mono-age stellar populations in three edge-on lenticular galaxies (FCC 153, FCC 170, and FCC 177) in the Fornax cluster, using deep MUSE observations. By measuring the half-mass radius (R_{50}) and half-mass height (z_{50}) across 1 Gyr-wide age bins, we trace the spatial evolution of stellar populations over cosmic time. All galaxies exhibit a remarkably constant disc thickness for all stars younger than $\sim$ 6 Gyr, suggesting minimal secular heating and limited impact from environmental processes such as tidal shocking or harassment. Evidence of past mergers (8–10 Gyr ago) is found in the increase of z_{50} for older populations. We find that accreted (metal-poor) stars have been deposited in quite thick configurations, but that the interactions only moderately thickened pre-existing stars in the galaxies, and only caused mild flaring in the outer regions of the discs. The radial structure of the discs varies across galaxies, but in all cases we find that the radial extent of mono-age populations remains constant or grows over the past 8 Gyr. This leads us to argue that within the radial range we consider, strangulation, rather than ram-pressure stripping, is the dominant quenching mechanism in those galaxies. Our results highlight the usefulness of analysing the structure of mono-age population to uncover the mechanisms driving galaxy evolution, and we anticipate broader insights from the GECKOS survey, studying 36 nearby edge-on disc galaxies.

Fornax3D, MUSE

IC 335

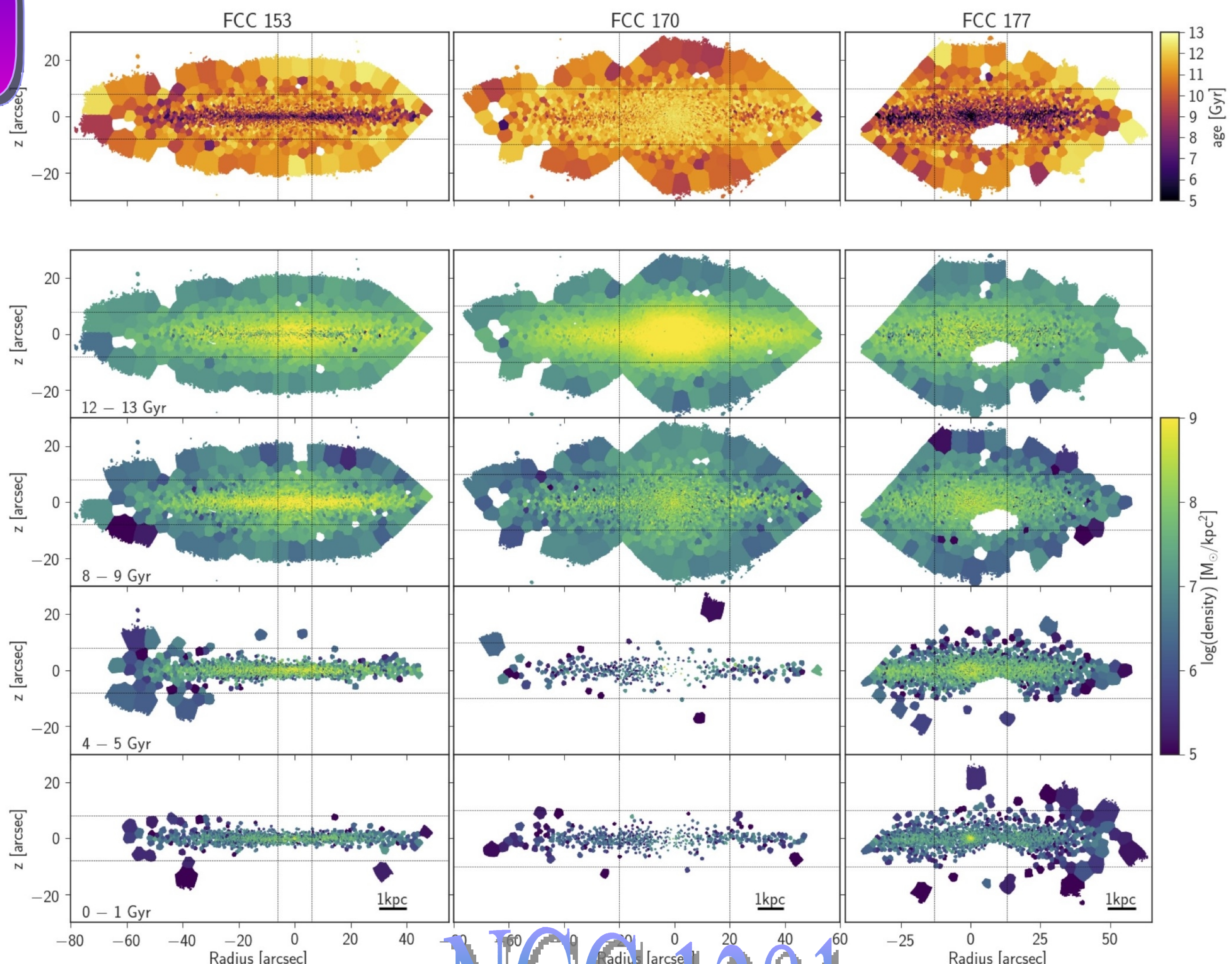

NGC 1381

Figure 1. The top row shows the average mass-weighted age distributions for the three galaxies studied here, while the rest of the figure shows the surface density for four different mono-age populations in each galaxy (12–13 Gyr old, 8–9 Gyr old, 4–5 Gyr old, and finally 0–1 Gyr old). In all panels, the vertical lines enclose the central bulge or bar-dominated region, while the horizontal lines delimitate the thin- and thick disc-dominated regions (Pinna et al. 2019a,b). In all galaxies, we find strong differences in the spatial distribution of stars of different ages: one striking aspect is the much thinner distribution of young stars compared to older stars.

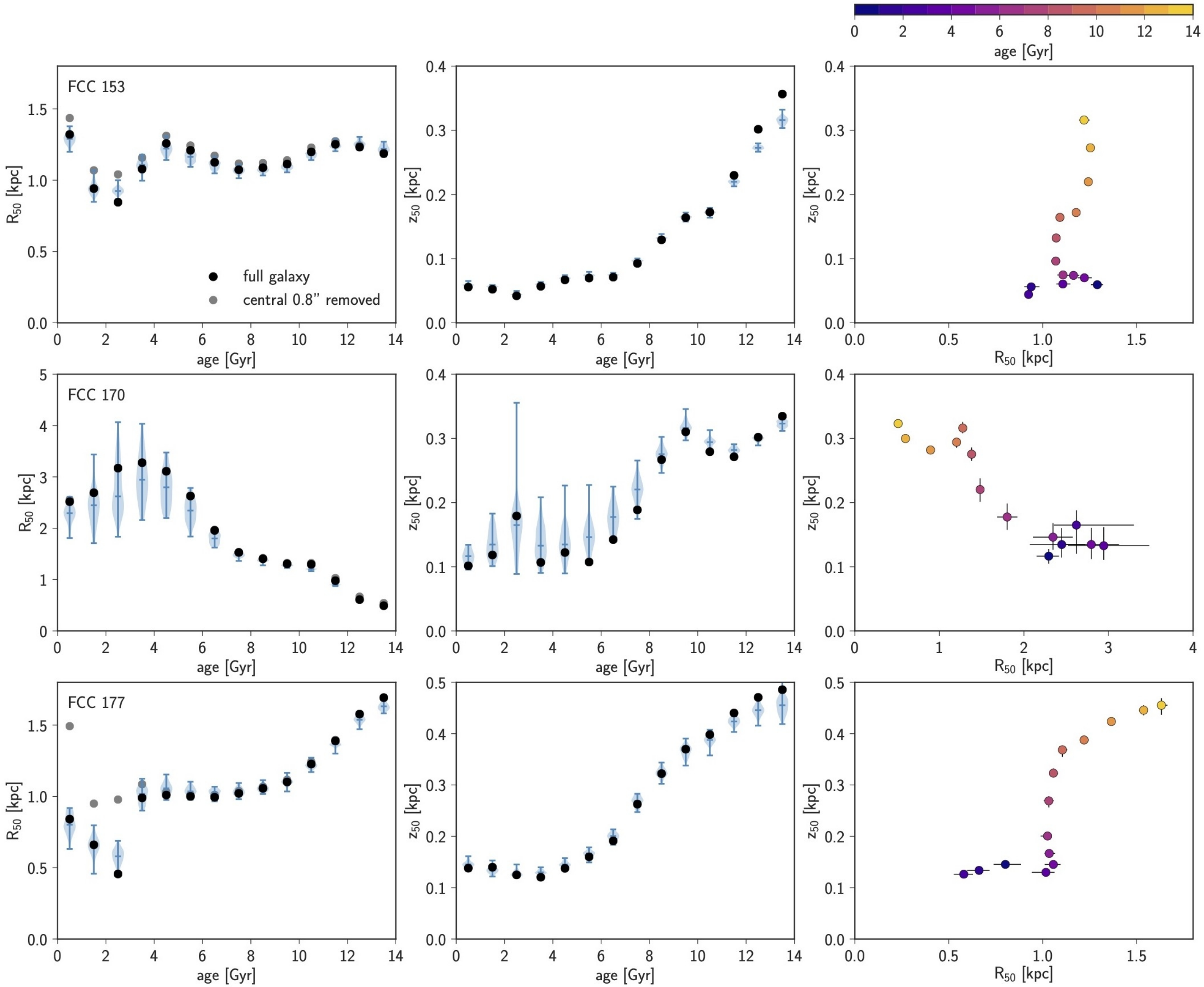

Figure 2. The first and second columns show R_{50} and z_{50} as a function of age for FCC 153, FCC 170 and FCC 177. The black dots represent the values obtained from our best fit to the spectra, while the blue violin plots represent the distribution of values obtained from the 50 Monte Carlo iterations (the upper and lower limits of the violin plots correspond to the full range of values from the 50 iterations, while the shape of the blue region represents the distribution of the values). The grey dots represent the values from the best fits, but excluding the very central regions of the galaxies, where nuclear star clusters are found. The third column represents z_{50} as a function of R_{50}, color-coded by age, for each galaxy. Here, the error bars represent the 16[th]-84[th] percentile range.

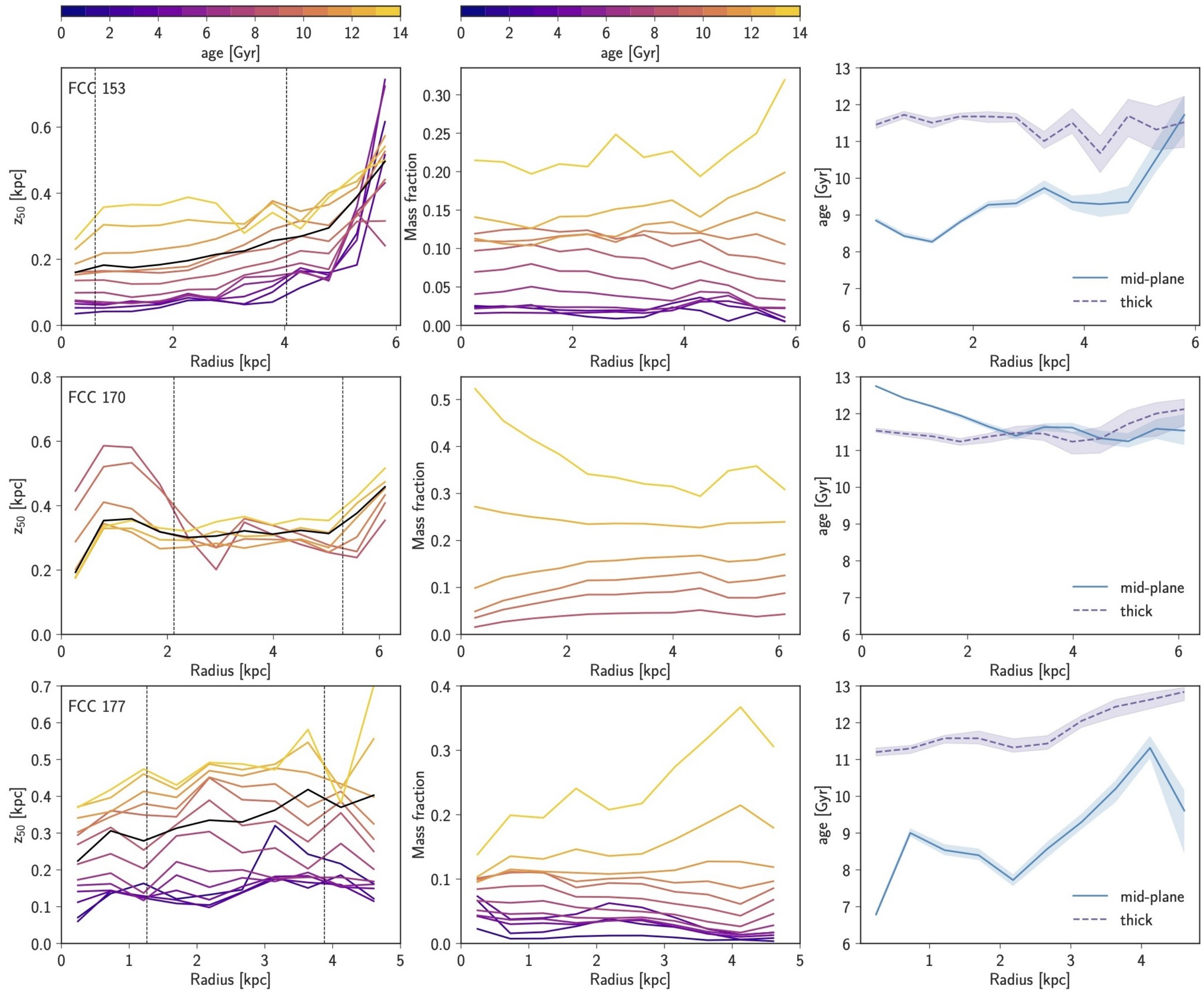

Figure 3. Structure of FCC 153 (top row), FCC 170 (middle) and FCC 177 (bottom). The first column shows radial profiles of z_{50} for mono-age populations, with each line color-coded by the age of the corresponding population. The thick black line represents the radial evolution of the global z_{50} for each galaxy. The vertical dashed lines delimit the regions of the galaxies we use to compute the mean z_{50} values shown in Fig. 2. The second column shows the mass fraction in each mono-age population, at each radius. In this column as in the first one, we only plot populations containing at least 1 per cent of the total mass of each galaxy. The last column shows radial profiles of the average mass-weighted age along the mid-plane (blue solid line) and the thick disc (violet dashed line). The shaded area represents the 16-84th percentile range, and the line the median.

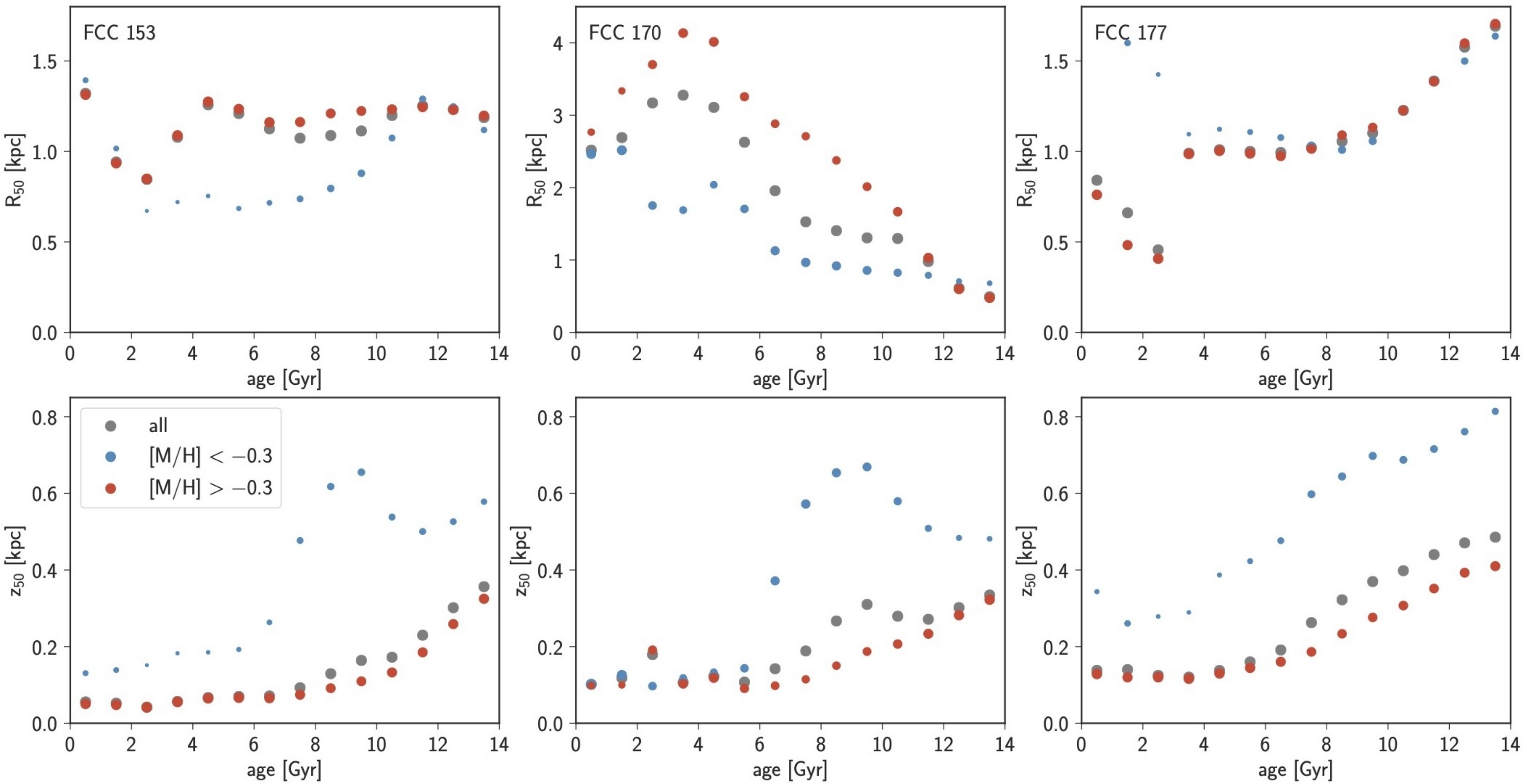

Figure 4. R_{50} (top row) and z_{50} (bottom row) as a function of age for FCC 153, FCC 170 and FCC 177. The grey dots represent the values obtained for the global population (they are the same as the black dots in Fig. 2), while the blue and red dots correspond to metal-poor and metal-rich stars, respectively. The surface of each blue and red dot is proportional to the fraction of the mass in this metallicity range at a given age. Pinna et al. (2019a,b) proposed that the 8–11 Gyr old metal-poor stars could be accreted from small galaxies: we indeed find that these stars have a different spatial distribution compared to the metal-rich stars (possibly formed in-situ).

Вывод:

- В последние (6?) миллиардов лет толщина и радиус звездных дисков в этих S0 не менялись.
- Значит: остановка звездообразования при входе в скопление не связана с лобовым давлением горячего газа (которое обрубает внешние части газового диска).
- Скорее всего, просто «голодание».

ArXiv: 2511.21187

Molecular Gas and Star Formation in Dwarf Galaxies Observed by the Atacama Large Millimeter/submillimeter Array

Kijeong Yim[1] and Soo-Chang Rey[1]

[1] *Department of Astronomy and Space Science, Chungnam National University, Daejeon 34134, Republic of Korea*

(Received August 19, 2025; Accepted November 15, 2025)

ABSTRACT

We present a spatially resolved analysis of the molecular star formation law (SFL) and gravitational instability in a sample of nearby dwarf galaxies (NGC 1035, NGC 4310, NGC 4451, NGC 4701, NGC 5692, and NGC 6106), using high-resolution ^{12}CO ($J = 1 \rightarrow 0$) data from the Atacama Large Millimeter/submillimeter Array. We estimate the star formation rate (SFR) by combining the Galaxy Evolution Explorer near-ultraviolet and the Wide-field Infrared Survey Explorer 12 μm imaging data to examine the relationship between molecular gas and SFR densities on scales of several hundred parsecs. We find that the power-law slope of the molecular SFL ranges from 0.62 to 1.08, with an average value of N$= 0.81 \pm 0.18$, increasing to N$= 0.87 \pm 0.05$ when excluding galaxies with poorly constrained CO data. These results are roughly consistent with values observed in massive spiral galaxies, suggesting a universal molecular SFL when analyzed with sufficient resolution and sensitivity. Radial profiles of the Toomre Q parameter remain close to unity across the disks, with minimal radial variation, consistent with a self-regulated star formation model. Our results suggest that, despite their lower mass and metallicity, star formation in dwarf galaxies is governed by the same fundamental physical processes as in larger systems. This highlights the significance of high-resolution molecular gas observations in low-mass galaxies.

Нашли в архиве 6 карликов, у которых закартирован CO:

Table 1. Galaxy Properties

Galaxy	R.A. (J2000) (h m s)	Decl. (J2000) (° ′ ″)	Morphology	PA (°)	Inclination (°)	Distance (Mpc)	$\log M_*$ ($M_\odot$)	R_{25} (′)	M_B (mag)
(1)	(2)	(3)	(4)	(5)	(6)	(7)	(8)	(9)	(10)
NGC 1035	02 39 29.1	−08 07 58.6	SAc	148	79	15.9	9.5	1.04	-18.3
NGC 4310	12 22 26.3	+29 12 31.2	SAB	158	71	16.1	9.3	0.97	-17.4
NGC 4451	12 28 40.6	+09 15 32.1	Sbc	158	49	25.9	9.7	0.67	-17.7
NGC 4701	12 49 11.6	+03 23 19.4	SAcd	45	49	16.7	9.4	0.87	-18.4
NGC 5692	14 38 18.1	+03 24 36.8	S	38	53	25.4	9.3	0.48	-19.0
NGC 6106	16 18 47.2	+07 24 39.2	SAc	141	59	24.3	9.7	1.09	-19.2

Note—Columns: (1) galaxy name; (2) and (3) galaxy coordinates; (4) morphological type of the galaxies from the NASA/IPAC Extragalactic Database (NED[a]); (5) position angle obtained from the *Spitzer* 3.6 μm or WISE 3.4 μm (only for NGC 5692) images using the MIRIAD task `IMFIT`; (6), (7), and (8) inclination, distance, and the total stellar mass from L. H. Cooke et al. (2022); (9) optical diameter in arcminutes from HyperLEDA[b] (D. Makarov et al. 2014); (10) absolute B magnitude from P. N. Truong et al. (2017).

Карты CO

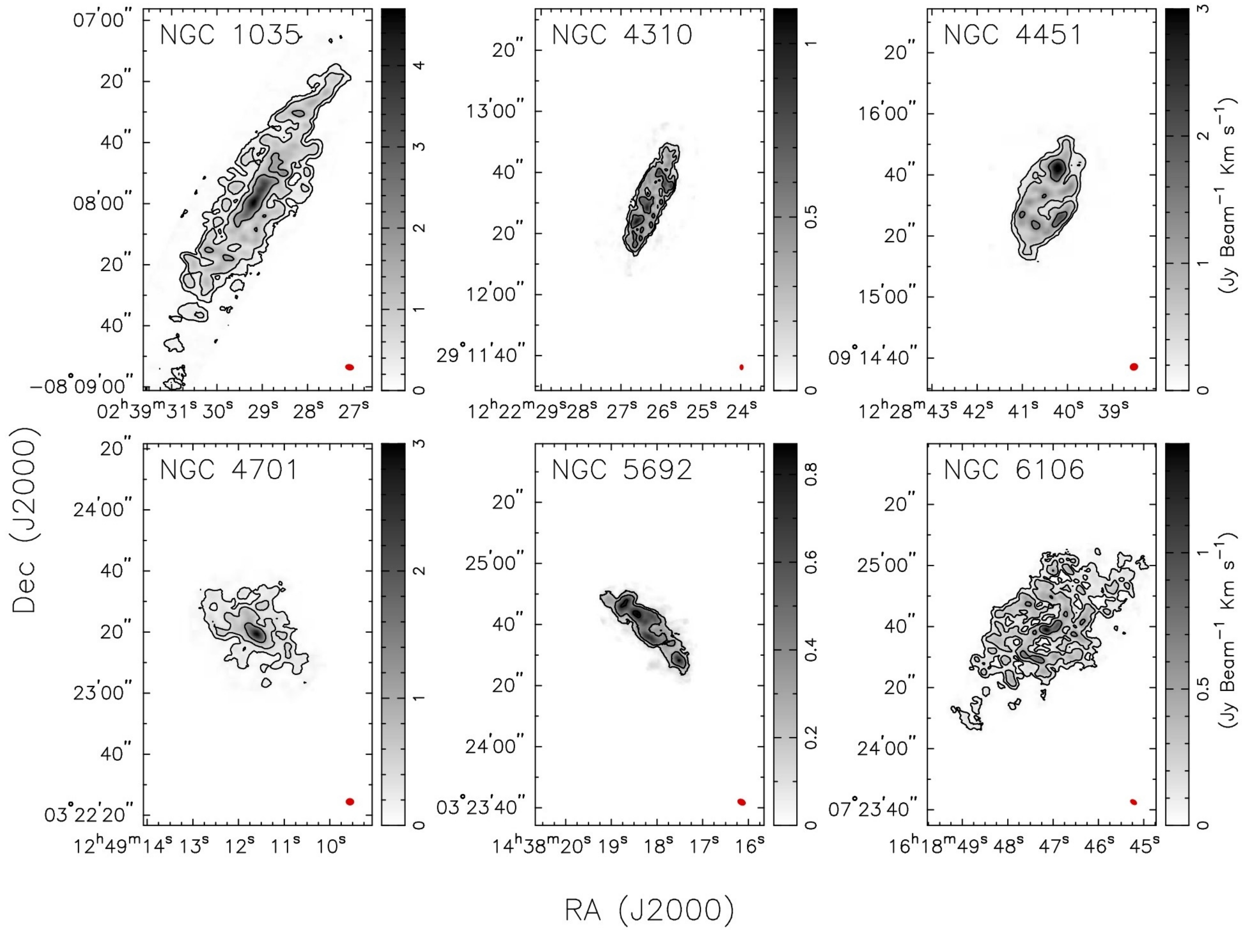

Figure 1. CO integrated intensity maps for the dwarf galaxies in our sample. Contour levels begin at approximately 5σ to clearly delineate reliable molecular gas detections. The synthesized beam size is indicated by the ellipse in the lower-right corner of each panel.

Карты звездной плотности

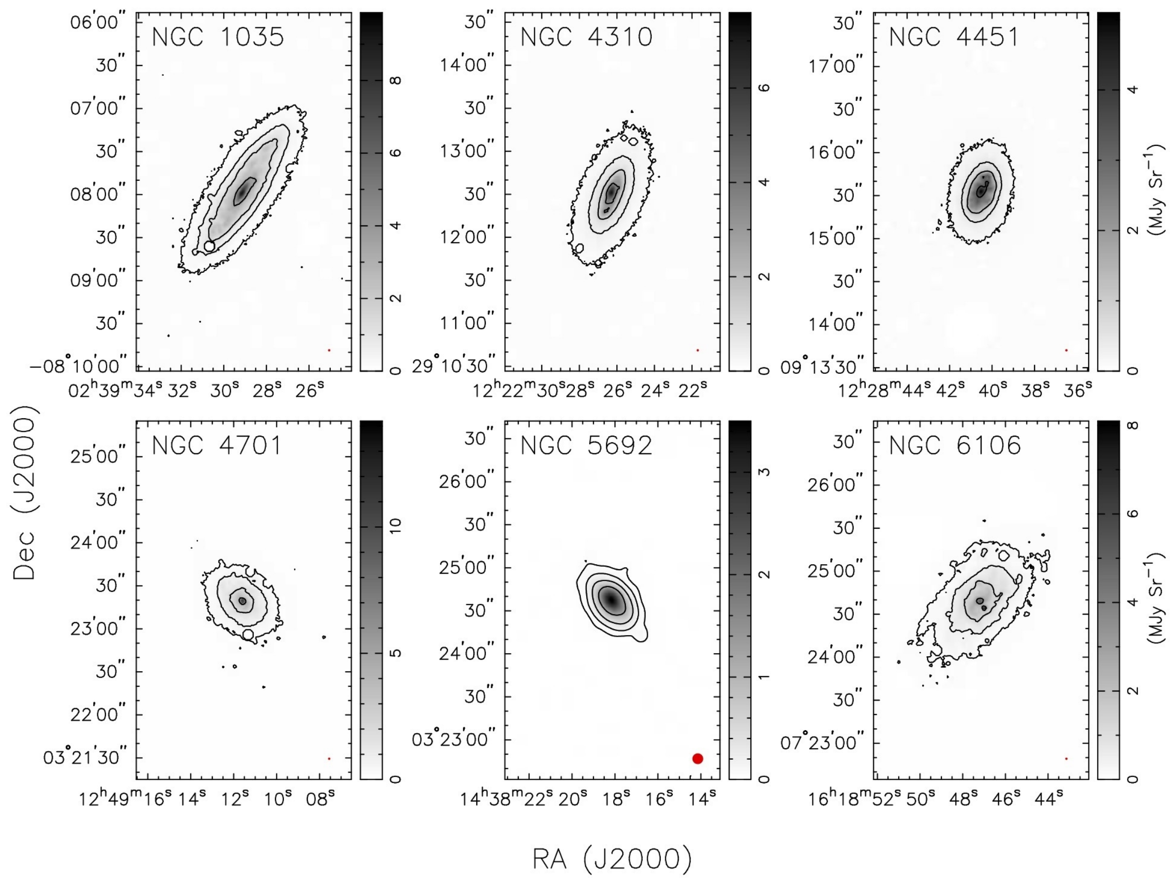

Figure 2. NIR images used to trace stellar mass distributions. For NGC 5692, the WISE 3.4 μm image is shown, while *Spitzer* IRAC 3.6 μm images are displayed for all other galaxies. The contours represent regions of significant stellar emission, beginning at approximately 15σ. The point spread function of the images is marked by the ellipse in the lower-right corner of each panel, illustrating the differences in spatial resolution between the WISE (7.″5) and *Spitzer* (1.″6) images.

Карты темпов звездообразования

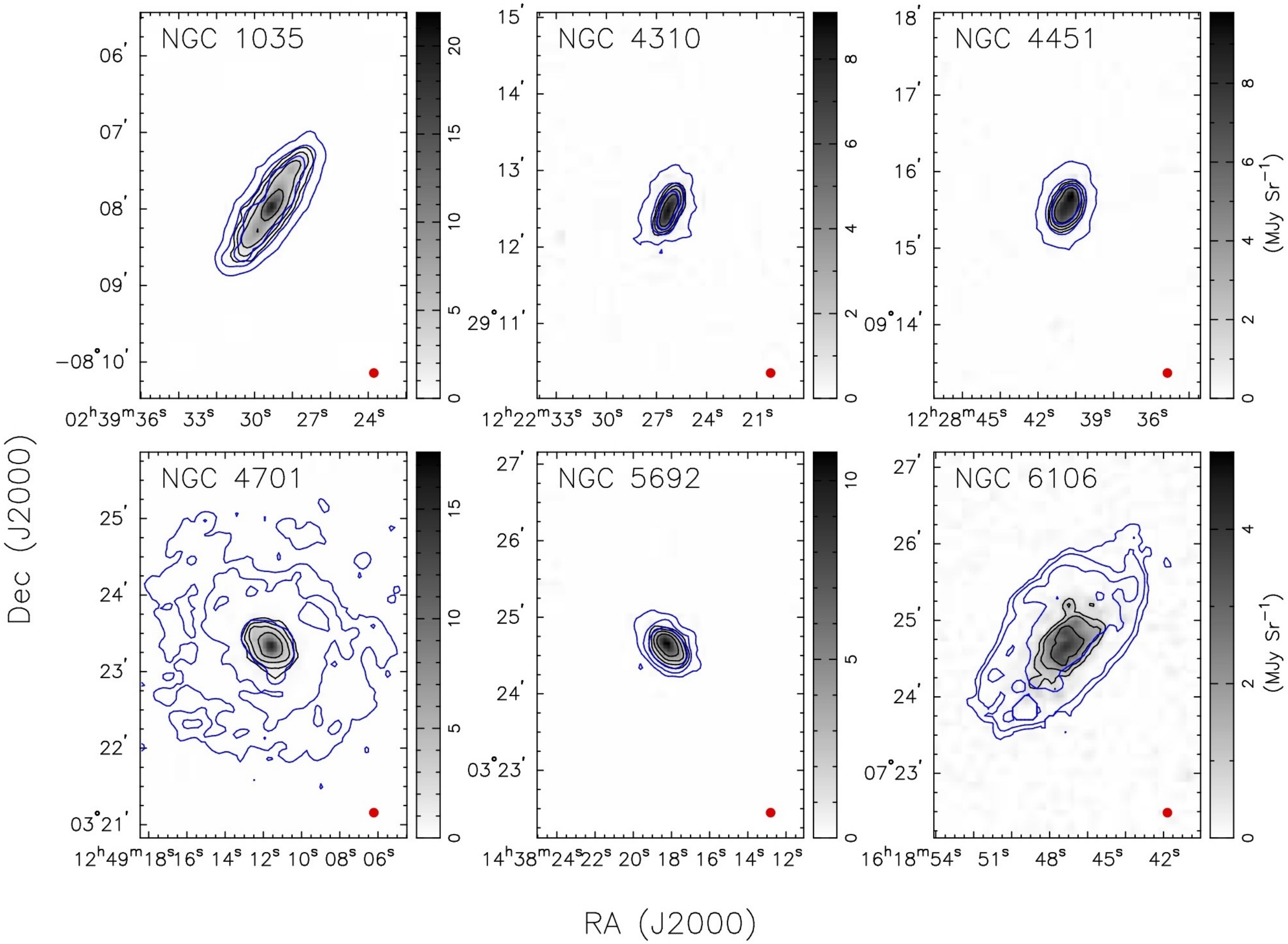

Figure 3. WISE 12 μm images and contours (black) for our dwarf galaxy sample, overlaid with contours from the GALEX NUV emission (blue). The lowest contour level for both 12 μm and NUV emissions is approximately 10σ. The PSF, with a Gaussian FWHM of $7''.5$, is makred by the ellipse in the lower-right corner of each panel.

… и радиальные профили всего

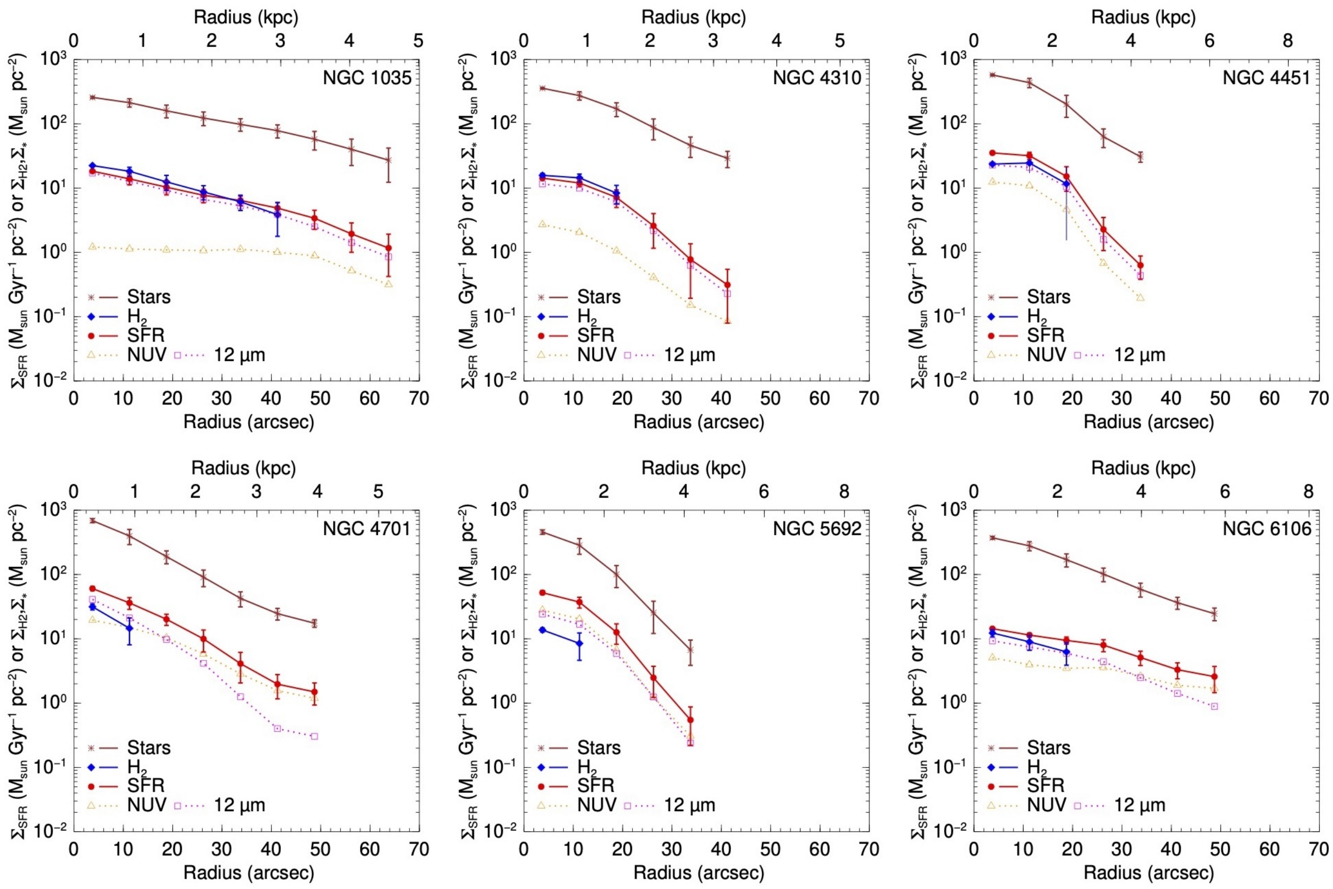

Figure 4. Radial surface density profiles of H_2 (blue diamonds), stars (brown stars), SFR (red circles), along with the individual contributions to the total SFR from NUV (orange triangles) and 12 μm (magenta squares). All profiles are measured in concentric elliptical annuli, each with a fixed radial width of 7.5″. The vertical error bars represent the standard deviation of data points in each annulus.

Физика звездообразования= как у спиральных галактик, N~1 (0.8)

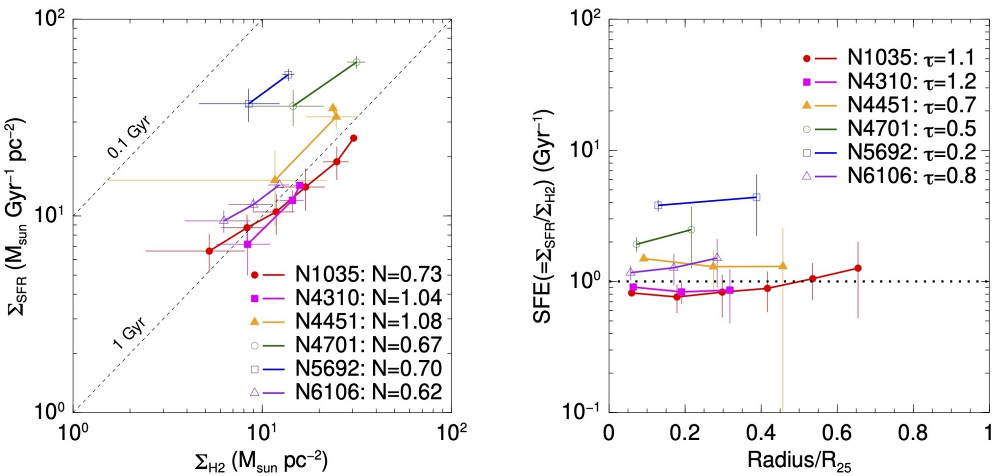

Figure 5. (Left) Relationship between $\Sigma_{\rm SFR}$ and $\Sigma_{\rm H_2}$ for the six dwarf galaxies. The dashed diagonal lines represent constant molecular gas depletion times (τ_{H_2}) of 0.1 and 1 Gyr for reference. The best-fit power-law index (N) is shown in the lower-right corner. (Right) SFE of the molecular gas ($\rm SFE_{H_2}$) as a function of radius normalized by the optical radius ($\rm R_{25}$). The molecular gas depletion time (τ_{H_2}), measured in Gyr, is indicated for each galaxy in the upper-right corner. The horizontal dotted line marks $\tau_{H_2} = 1$ Gyr as a reference point.

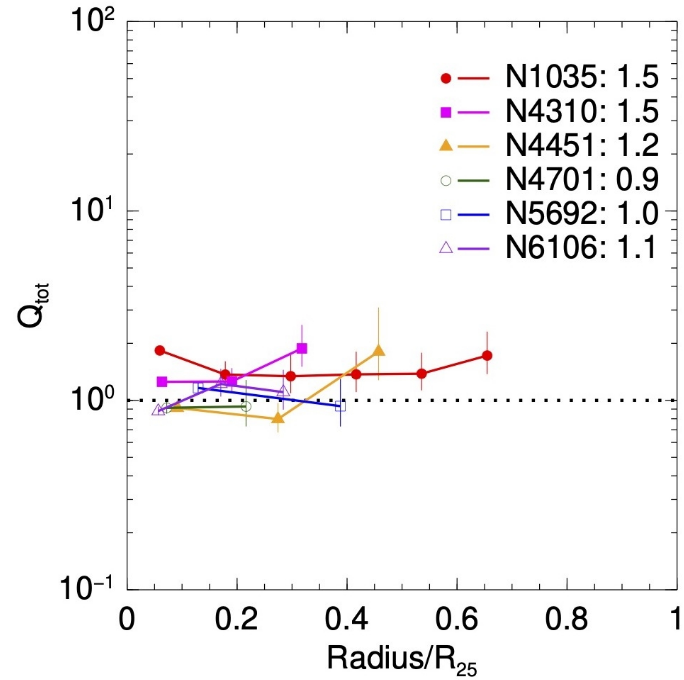

Figure 6. $Q_{\rm tot}$ as a function of radius, normalized by the optical radius R_{25} for the six dwarf galaxies. The horizontal line at $Q_{\rm tot} = 1$ marks the threshold for gravitational instability; regions below the line are dynamically unstable and susceptible to star formation.

Количественные выводы:

- Q~1
- N=0.81+/-0.18